Deletion of Macrophage Mineralocorticoid Receptor Protects Hepatic Steatosis and Insulin Resistance Through ERα/HGF/Met Pathway

Yu-Yao Zhang,[1,2,3] Chao Li,[1,2,3] Gao-Feng Yao,[3] Lin-Juan Du,[1,2,3] Yuan Liu,[1,2,3] Xiao-Jun Zheng,[1,2,3] Shuai Yan,[3] Jian-Yong Sun,[3] Yan Liu,[1,2] Ming-Zhu Liu,[3] Xiaoran Zhang,[4] Gang Wei,[4] Wenxin Tong,[5] Xiaobei Chen,[5] Yong Wu,[6,7] Shuyang Sun,[2,8] Suling Liu,[9] Qiurong Ding,[3] Ying Yu,[10] Huiyong Yin,[3] and Sheng-Zhong Duan[1,2]

Although the importance of macrophages in nonalcoholic fatty liver disease (NAFLD) and type 2 diabetes mellitus (T2DM) has been recognized, how macrophages affect hepatocytes remains elusive. Mineralocorticoid receptor (MR) has been implicated to play important roles in NAFLD and T2DM. However, cellular and molecular mechanisms are largely unknown. We report that myeloid MR knockout (MRKO) improves glucose intolerance, insulin resistance, and hepatic steatosis in obese mice. Estrogen signaling is sufficient and necessary for such improvements. Hepatic gene and protein expression suggests that MRKO reduces hepatic lipogenesis and lipid storage. In the presence of estrogen, MRKO in macrophages decreases lipid accumulation and increases insulin sensitivity of hepatocytes through hepatocyte growth factor (HGF)/Met signaling. MR directly regulates estrogen receptor 1 (*Esr1* [encoding ERα]) in macrophages. Knockdown of hepatic Met eliminates the beneficial effects of MRKO in female obese mice. These findings identify a novel MR/ERα/HGF/Met pathway that conveys metabolic signaling from macrophages to hepatocytes in hepatic steatosis and insulin resistance and provide potential new therapeutic strategies for NAFLD and T2DM.

Nonalcoholic fatty liver disease (NAFLD) is intimately intertwined with insulin resistance and type 2 diabetes mellitus (T2DM). The ectopic lipid accumulation in hepatocytes in the process of NAFLD directly or indirectly impairs key components of the insulin signaling pathway and markedly increases the risk of T2DM (1,2). Insulin resistance and T2DM, on the other hand, impair hepatic metabolism and exacerbate NAFLD. With the increasing prevalence of T2DM, NAFLD affects more and more individuals worldwide.

Kupffer cells (KCs) and their interactions with hepatocytes play essential roles in hepatic steatosis and insulin resistance. KCs are a group of specific macrophages that reside in the liver. Depletion of KCs improves hepatic steatosis and insulin resistance (3). Given the evolutionary homology, KCs and hepatocytes are situated in proximity

METABOLISM

---

[1]Laboratory of Oral Microbiology, Shanghai Research Institute of Stomatology, Ninth People's Hospital, School of Stomatology, Shanghai Jiao Tong University School of Medicine, Shanghai, China

[2]Shanghai Key Laboratory of Stomatology, Shanghai Jiao Tong University School of Medicine, Shanghai, China

[3]Key Laboratory of Nutrition and Metabolism, Institute for Nutritional Sciences, Shanghai Institutes for Biological Sciences, Chinese Academy of Sciences, University of the Chinese Academy of Sciences, Shanghai, China

[4]Key Laboratory of Computational Biology, CAS-MPG Partner Institute for Computational Biology, Shanghai Institutes for Biological Sciences, Chinese Academy of Sciences, Shanghai, China

[5]Department of Infectious Diseases, Ren-Min Hospital of Wuhan University, Wuhan, China

[6]Division of Cancer Research and Training, Department of Internal Medicine, Charles R. Drew University of Medicine and Science, Los Angeles, CA

[7]David Geffen School of Medicine at University of California Los Angeles, Los Angeles, CA

[8]Department of Oral and Maxillofacial-Head Neck Oncology, Ninth People's Hospital, Shanghai Jiao Tong University School of Medicine, Shanghai, China

[9]Shanghai Cancer Center and Institutes of Biomedical Sciences, Key Laboratory of Breast Cancer in Shanghai, Cancer Institute, Fudan University, Shanghai, China

[10]Department of Pharmacology, School of Basic Medical Sciences, Tianjin Medical University, Tianjin, China

Corresponding author: Sheng-Zhong Duan, duansz@shsmu.edu.cn.

Received 4 November 2016 and accepted 13 March 2017.

with each other in the liver, allowing efficient communications between these cell types (4). Studies have focused on inflammation as the link from KCs to hepatocytes, although the key connections are still elusive. For instance, tumor necrosis factor-α has been implicated as such a connecting point (3). However, macrophage tumor necrosis factor-α plays only negligible roles in hepatic steatosis and insulin resistance (5). Moreover, much less is known about the impacts of macrophage-derived metabolic factors on hepatocytes. These metabolic factors may be particularly important in the early stage of simple hepatic steatosis without inflammation. Therefore, although the contribution of KCs has been recognized in hepatic steatosis and insulin resistance, the mechanisms mediating the signals from KCs to hepatocytes remain largely unknown.

Mineralocorticoid receptor (MR) may regulate the interactions between macrophages and hepatocytes and therefore play important roles in hepatic steatosis and insulin resistance. MR is a member of the nuclear receptor superfamily. Its functions in the cardiovascular system have been explored (6,7), and MR antagonists are already in clinical use to treat heart failure (8). Antagonists of MR also have been shown to improve hepatic steatosis and insulin resistance in animal models of obesity (9–12), supporting the metabolic benefits of MR blockade. However, little is known about the cellular and molecular mechanisms. Given the importance of macrophages, the role of macrophage MR and whether MR controls metabolic factors and related signaling pathways that regulate macrophage-hepatocyte interaction in the setting of hepatic steatosis and insulin resistance are of great interest.

In this study, we determined whether and how macrophage MR deletion affects hepatic steatosis and insulin resistance. We first studied the effects of myeloid MR knockout (MRKO) on insulin sensitivity, glucose homeostasis, and hepatic steatosis by using obese mouse models. We then explored the impacts of MRKO in macrophages on lipid accumulation and insulin sensitivity of hepatocytes by using a coculture system. Finally, we deciphered the molecular basis and delineated a new signaling pathway involving MR/estrogen receptor-α (ERα)/hepatic growth factor (HGF) and conveyed messages from macrophages to hepatocytes through Met both in culture and in mice.

RESEARCH DESIGN AND METHODS

Animals
Floxed control (FC) and myeloid MRKO mice were generated as previously described (13) and crossed with $Lep^{ob/wt}$ mice on a C57BL/6 background (The Jackson Laboratory) to obtain the following four experimental groups: FC ($MR^{fl/fl}$), MRKO ($MR^{fl/fl}$::LysM-cre), FC-ob ($MR^{fl/fl}$::$Lep^{ob/ob}$), and MRKO-ob ($MR^{fl/fl}$::LysM-cre::$Lep^{ob/ob}$). For 17β-estradiol (E$_2$) treatment, 4-week-old male obese mice were implanted with E$_2$ pellets (0.18 mg/pellet; Innovative Research) or placebo subcutaneously as previously described (14). All animal protocols were approved by the Institutional Review and

Ethics Board of the Ninth People's Hospital, Shanghai Jiao Tong University School of Medicine, and the Institutional Animal Care and Use Committee of the Institute for Nutritional Sciences, Shanghai Institutes for Biological Sciences, Chinese Academy of Sciences (Shanghai, China).

Glucose and Insulin Tolerance Tests
Glucose tolerance test (GTT) was performed in 10-week-old *ob/ob* mice with intraperitoneal injection of 1 g/kg glucose after an 8-h fasting. Insulin tolerance test (ITT) was conducted in 11-week-old *ob/ob* mice with intraperitoneal injection of insulin (1 unit/kg) after a 5-h fasting. For experiments with hepatic Met knockdown, GTT and ITT were performed 3 and 5 days after injection of adenoviruses, respectively.

Tissue Sample Collection
Twelve-week-old *ob/ob* mice were anesthetized after 5 h of fasting followed by tissue dissection as previously described (15). Briefly, after blood collection, insulin (5 units/kg) was injected into the inferior vena cava. Liver, uterine adipose tissue, and skeletal muscle were collected and snap-frozen in liquid nitrogen 3, 4, and 5 min after insulin injection, respectively. Tissues were also collected before insulin injection. For experiments with hepatic Met knockdown, random-fed blood glucose was measured 4 days after and tissues collected 7 days after adenovirus injection. Additional blood samples were taken from 11-week-old mice fed ad libitum for insulin measurements.

Histology
Hepatic hematoxylin-eosin (H&E) staining was performed as previously described (16). Oil Red O staining was carried out as previously reported (17), and quantification was performed with Image J software.

Measurement of Triglycerides and Free Fatty Acids
Plasma concentrations of triglycerides (TGs) and free fatty acids (FFAs) were determined by using an automated biochemical analyzer at the Xuhui District Central Hospital (Shanghai, China). To measure hepatic TG and FFA content, lipid extract was prepared and dissolved as previously reported (18). The concentration of TGs was measured at the Xuhui District Central Hospital. TG content was normalized with tissue weight. Hepatic FFAs were measured by gas chromatography-mass spectrometry profiling.

Immunoblotting
Total protein was extracted from frozen tissues or cultured cells. Quantified protein was separated by SDS-PAGE, transferred onto polyvinylidene fluoride membranes, and immunoblotted with primary antibodies and secondary antibodies sequentially. Membranes were visualized by using ECL Western Blotting Substrate (Thermo Fisher Scientific). Band intensity was quantified by using Quantity One software (Bio-Rad) and normalized to total protein or α-tubulin.

The following primary antibodies were used: anti-insulin receptor (IR) (3025S), antiphospho-IR (3024S), anti-Akt (9272S), antiphospho-Akt (Ser473, 9271S), anti-Met (3127), antiphospho-Met (3126S), anti-acetyl-CoA

carboxylase (ACC) (3662), and anti-stearoyl-CoA desaturase 1 (SCD-1) (2438) from Cell Signaling Technology; anti-α-tubulin (T6199) and anti-FLAG (F3165) from Sigma-Aldrich; anti-cell death–inducing DNA fragmentation factor-α–like effector a (Cidea) (ab8402) from Abcam; anti-lymphocyte antigen 6 complex, locus D (Ly6d) (17361–1-AP) from Proteintech; and anti-MR (sc-11412) and anti-fatty acid synthase (FAS) (sc-48357) from Santa Cruz Biotechnology.

Lipidomics

Lipid extraction and processing was performed as previously described (19). A derivatization method was used to improve specificity and sensitivity of phosphatidylethanolamine (PE) detection (20). The shotgun lipidomics was carried out with a TSQ Vantage triple quadrupole mass spectrometer (Thermo Fisher Scientific) according to published protocols (21). Tandem mass spectrometry scan fragment and collision energy for each lipid class were optimized according to previously published methods (21).

Cell Culture

Mouse primary hepatocytes were isolated by in situ collagenase perfusion as previously described, with minor modifications (22). The cell suspension was further purified with 50% Percoll (GE Healthcare) before counting and plating.

KCs were isolated from female mice as previously reported, with minor modifications (23). After 25–50% Percoll gradient centrifugation, the KC-enriched interlayer was collected and plated. Nonadherent and floating cells were washed off 15–30 min after plating. In a separate experiment, KCs were preincubated with 0.1 μmol/L ICI 182,780 (Tocris Bioscience) for 24 h and then with 10 nmol/L E_2 for another 24 h in the presence or absence of ICI 182,780.

For hepatocyte-KC coculture, hepatocytes and KCs were plated successively at a ratio of 10:1, and incubated with 10 nmol/L E_2 for 5 h after overnight recovery. The cells were then stimulated with FFAs (a combination of 200 μmol/L oleic acid and 100 μmol/L palmitic acid) in the presence of E_2. For insulin-stimulated effects, insulin (100 nmol/L) was added to the media after coculture for 20 min.

ELISA

Plasma insulin concentration was determined by Rat Ultrasensitive Insulin ELISA kit (ALPCO). HGF levels were determined by using Mouse/Rat HGF Quantikine ELISA Kit (R&D Systems) according to the manufacturer's instructions. Plasma E_2, dihydrotestosterone, and testosterone levels were measured by using kits from DRG International (EIA-4399 and EIA-5761) and Enzo Life Sciences (ADI-900-065) according to the manufacturers' protocols.

Met Knockdown in Primary Hepatocytes

Primary hepatocytes were transfected with Met small interfering RNA (siRNA) (GenePharma) by using X-tremeGENE siRNA Transfection Reagent (Roche Diagnostics) according to the manufacturer's instructions. The sequences of the Met siRNA were: GGAGGUGUUUGGAAAGAUATT, UAUCUUUCCAAACACCUCCTG.

Establishment of a Stable MR Overexpression RAW264.7 Cell Line

A stable MR overexpression (MROV) RAW264.7 cell line was established as previously described (16). The full-length mouse Mr3c2 coding region was amplified and subcloned into pHAGE-fEF1a-IRES-ZsGreen vector for subsequent transfection.

Construction of Truncated Mouse Esr1 Promoter Luciferase Reporter Plasmids

A 2-kilobase pair (kb) mouse estrogen receptor 1 (Esr1) promoter was amplified and cloned into pGL3-basic vector (Promega) to produce the 2-kb Esr1-luciferase plasmid. Specific primers were used to yield various truncated Esr1-luciferase plasmids. Sequences of these primers are listed in Supplementary Table 1.

Chromatin Immunoprecipitation

Chromatin immunoprecipitation (ChIP) experiments were performed in MROV RAW264.7 cells by using an EZ-ChIP kit (EMD Millipore) according to the manufacturer's protocols. Cells were cultured with DMEM containing 10% charcoal/dextran-treated FBS. Primer sequences for PCR analysis of ChIP products are listed in Supplementary Table 2.

Generation and Administration of Recombinant Adenoviruses

Recombinant adenoviruses were generated by using the BLOCK-iT Adenoviral RNAi Expression System (Thermo Fisher Scientific) according to the manufacturer's instructions. The adenoviruses were administered to 10-week-old female obese mice at a dose of 1×10^9 plaque-forming units/mouse through the tail vein (24). For cell culture experiments, purified adenoviruses were used at a dose of 1×10^7 plaque-forming units/well in 12-well plates. The sequence of scrambled short hairpin RNA (shRNA) was 5'-CCTAAGGTTAAGTCGCCCTCGCTC-3', the sequence of Met-specific shRNA was 5'-CGTGTTGGAACACCCAGATTGTTTA-3', and the sequence of ERα-specific shRNA was 5'-TACTACCTGGAGAACGAGCCCA-3'.

Statistical Analysis

All data are presented as mean ± SEM. Comparisons between groups were done by Student t test, and comparisons between curves were performed with two-way ANOVA and Bonferroni posttests with GraphPad Prism software. $P \leq 0.05$ was considered statistically significant.

RESULTS

Myeloid MR Deficiency Improves Glucose Homeostasis and Insulin Sensitivity in Female ob/ob Mice

We first used the ob/ob mouse model to study the impacts of myeloid MR deficiency on obesity and T2DM. Random-fed blood glucose of female MRKO-ob mice was drastically lower than that of FC-ob mice (Fig. 1A). Improved GTT and ITT were also observed in female MRKO-ob mice (Fig. 1B–E). Furthermore, female MRKO-ob mice had markedly lower fasting plasma insulin (Fig. 1F) and significantly lower
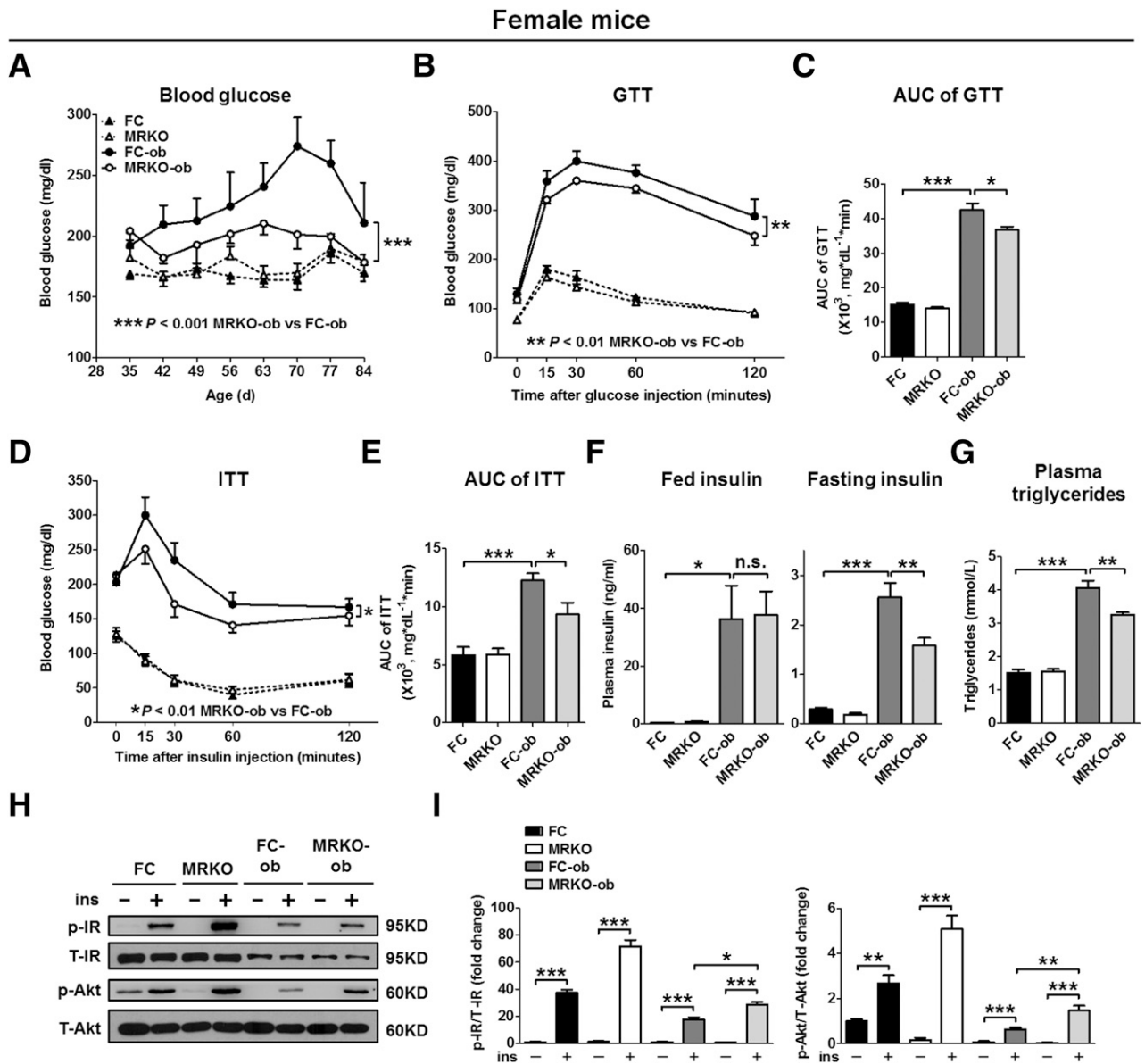
Female mice

Figure 1—Improved glucose homeostasis and insulin sensitivity in female MRKO-ob mice. A–E: Weekly random-fed blood glucose levels, GTT, area under the curve (AUC) of GTT, ITT, and AUC of ITT of female mice. F: Plasma insulin levels of fed or fasted female mice. G: Plasma TGs of female mice. H: Immunoblotting analysis of p-IR, total IR (T-IR), p-Akt (Ser473), and total Akt (T-Akt) in livers of female mice. I: Quantification of immunoblotting results as p-IR/T-IR and p-Akt/T-Akt. $n = 6–8$. $*P < 0.05$, $**P < 0.01$, $***P < 0.001$. −, before insulin injection; +, after insulin injection; n.s., not significant.

plasma TGs (Fig. 1G) than FC-ob mice. Female MRKO-ob and FC-ob mice had comparable body weights, body composition, food consumption, islet areas, and plasma FFAs (Supplementary Fig. 1A–F). Therefore, female MRKO-ob mice displayed improved insulin sensitivity and glucose homeostasis.

We then determined insulin sensitivity in major insulin target tissues of female mice. In liver, phosphorylation of IR (p-IR) and phosphorylation of Akt (p-Akt) were induced by insulin in both FC-ob and MRKO-ob mice, but a much larger increase was observed in MRKO-ob mice (Fig. 1H and I). In uterine adipose tissue and skeletal muscle,

insulin-stimulated p-IR and p-Akt were similar between the two genotypes (Supplementary Fig. 1G–J). These results imply that the improved systemic insulin sensitivity of MRKO-ob mice is mostly attributable to enhanced hepatic insulin responsiveness.

Myeloid MR Deficiency Improves Glucose Homeostasis and Insulin Sensitivity in Male *ob/ob* Mice Treated With Estrogen

In contrast to females, male MRKO-ob mice and FC-ob mice showed comparable metabolic parameters (Supplementary Fig. 2). In a model of high-fat diet (HFD)–induced obesity and insulin resistance, we did not observe a significant

difference between male FC and MRKO mice (Supplementary Fig. 3). In female mice, HFD failed to induce insulin resistance in either genotype, although body weight gain was observed (data not shown) consistent with previous results (25).

We next tested whether estrogen supplementation would influence the metabolic phenotype of male MRKO-ob mice. Eight weeks of E_2 treatment significantly improved random-fed blood glucose, GTT, ITT, fasting plasma insulin, and TGs in male FC-ob and MRKO-ob mice (Fig. 2A–G). Of note, many more improvements were detected in MRKO-ob

mice and as a result, E_2-implanted MRKO-ob mice had significantly more improved metabolic parameters than E_2-implanted FC-ob mice (Fig. 2A–G). No difference in body weight loss or hypophagia was observed between male FC-ob and MRKO-ob mice after E_2 treatment (data not shown). Hepatic insulin signaling was also markedly enhanced in E_2-implanted MRKO-ob mice compared with that of E_2-implanted FC-ob mice (Fig. 2H and I). E_2 implantation increased plasma E_2 and decreased plasma dihydrotestosterone and testosterone in male FC-ob and MRKO-ob mice to similar levels (Supplementary Fig. 4). Therefore,
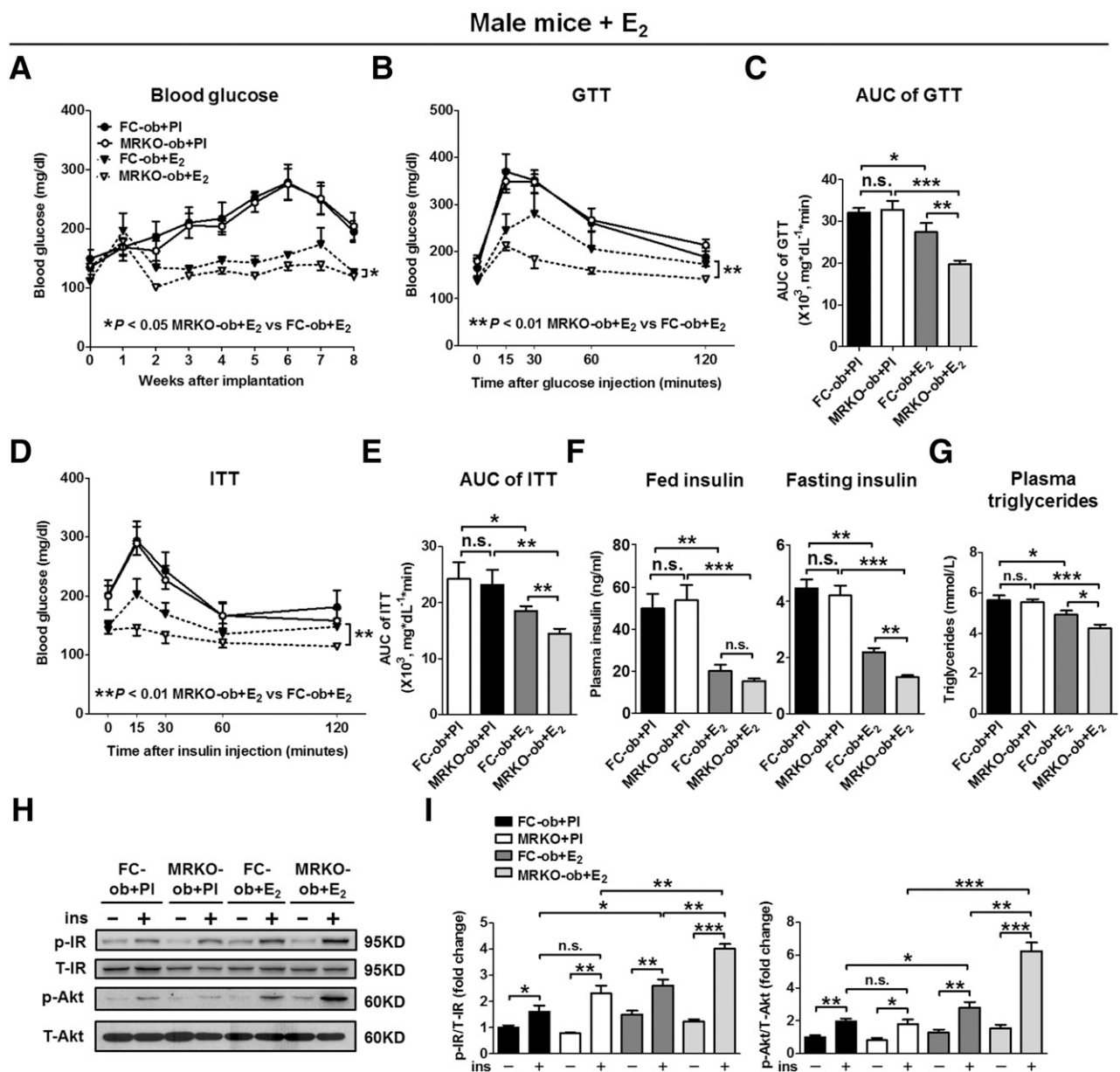
Figure 2—Improved glucose homeostasis and insulin sensitivity in male MRKO-ob mice treated with estrogen. A–E: Weekly random-fed blood glucose levels, GTT, area under the curve (AUC) of GTT, ITT, and AUC of ITT of male mice. F: Plasma insulin levels of fed or fasted male mice. G: Plasma TGs of male mice. H: Immunoblotting analysis of p-IR, total IR (T-IR), p-Akt (Ser473), and total Akt (T-Akt) in livers of male mice. I: Quantification of immunoblotting results as p-IR/T-IR and p-Akt/T-Akt. $n = 5$–7. *$P < 0.05$, **$P < 0.01$, ***$P < 0.001$. −, before insulin injection; +, after insulin injection; n.s., not significant; PI, placebo.

estrogen supplementation was sufficient to elicit metabolic protection of MRKO in male obese mice.

To test the necessity of estrogen for metabolic improvements, female obese mice underwent ovariectomy (OVX), which eradicated E_2 in the plasma of both female FC-ob and MRKO-ob mice (Supplementary Fig. 5A). OVX abolished the beneficial effects of MRKO in female obese mice (Supplementary Fig. 5B–E).

Collectively, myeloid MRKO improved insulin sensitivity, glucose homeostasis, and hepatic insulin signaling of obese mice. Estrogen was sufficient and necessary for myeloid MRKO-mediated metabolic protection.

Myeloid MR Deletion Attenuates Hepatic Steatosis in *ob/ob* Mice

Female MRKO-ob mice had a significantly lower liver weight-to-body weight ratio (LW/BW) than FC-ob mice (Fig. 3A). Histology of livers showed much smaller and fewer lipid droplets in female MRKO-ob mice (Fig. 3B). Furthermore, hepatic TG content was markedly reduced in female MRKO-ob mice compared with FC-ob mice (Fig. 3C).

In males, no obvious difference was observed in LW/BW or hepatic TG content between MRKO-ob and FC-ob mice (Supplementary Fig. 6A and B). Similarly, LW/BW of HFD-fed myeloid MRKO mice and that of HFD-fed FC mice were comparable (Supplementary Fig. 6C). After E_2 treatment, male MRKO-ob mice manifested decreased LW/BW, lipid droplets, and hepatic TG content compared with male FC-ob mice (Fig. 3D–F). In addition, LW/BW, lipid accumulation and hepatic TG content were comparable between female MRKO-ob and FC-ob mice after OVX (Supplementary Fig. 6D–F).

To investigate the contribution of lipid metabolites, we performed shotgun lipidomics to analyze subclasses of TGs and phospholipids in livers of female mice. The majority of the TG species were significantly downregulated in livers of female MRKO-ob mice compared with FC-ob mice, including the most abundant species C52:2, C52:3, and C54:3 (Fig. 3G). Total content of phosphatidylcholine (PC) were significantly reduced in livers of female MRKO-ob mice (Supplementary Fig. 7A). Consistently, the majority of the individual PC species were decreased in livers of MRKO-ob mice compared with FC-ob mice (Fig. 3H). No significant difference was found in other phospholipid classes between MRKO-ob and FC-ob mice (Supplementary Fig. 7A–C). In addition, hepatic fatty acids were reduced in MRKO-ob mice compared with FC-ob mice (Supplementary Fig. 7D–F). These data suggest that myeloid MRKO alleviates hepatic steatosis in female *ob/ob* mice, particularly by decreasing the content of TGs and fatty acids as well as altering the composition of phospholipid species.

Myeloid MR Deletion Downregulates Molecules Important in Hepatic Lipogenesis and Lipid Storage in Female *ob/ob* Mice

SCD-1 is a rate-limiting enzyme in hepatic de novo lipogenesis (26). Results of quantitative RT-PCR (qRT-PCR) demonstrated that hepatic expression of *SCD-1* was significantly
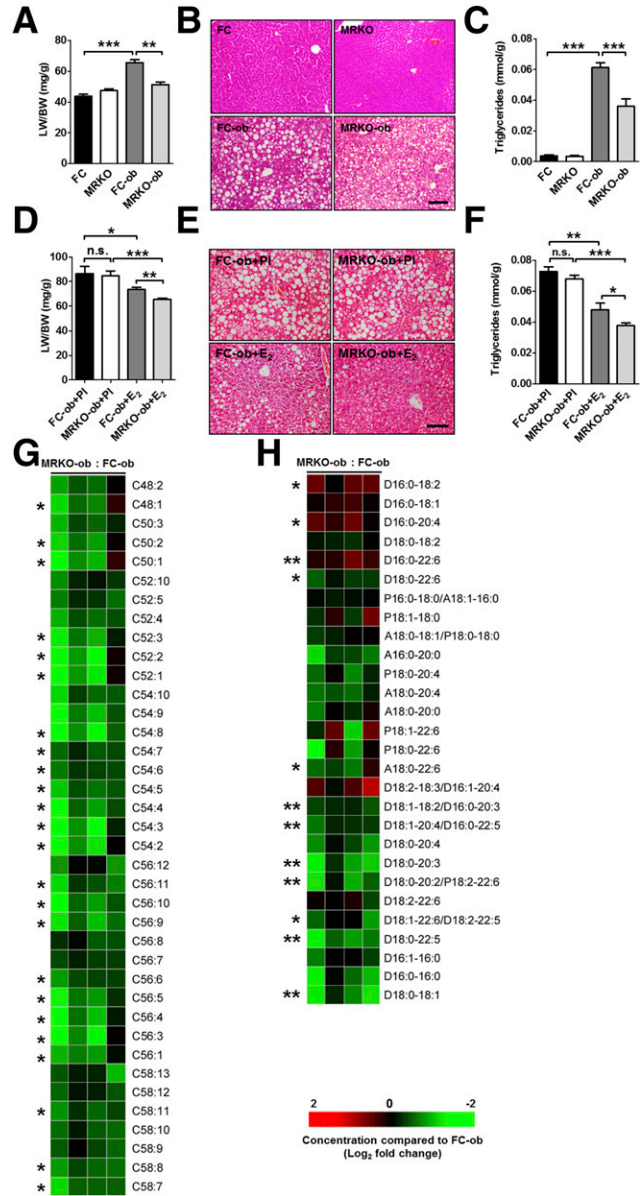
Figure 3—Attenuated hepatic steatosis in female and E_2-implanted male MRKO-ob mice. A and B: LW/BW and hepatic H&E staining of female mice ($n = 6–8$). Scale bar = 200 μm. C: Hepatic TGs of female mice ($n = 6–8$). D and E: LW/BW and hepatic H&E staining of male obese mice implanted with placebo (Pl) or E_2 ($n = 5–7$). Scale bar = 500 μm. F: Hepatic TGs of male obese mice implanted with Pl or E_2 ($n = 5–7$). G: Quantification of TG species based on lipidomic analysis of hepatic lipids extracted from female mice ($n = 4$). Data are ratios of the MRKO-ob value of each species relative to the mean value of FC-ob group after normalization with hepatic protein concentration. Red represents higher and green lower concentration in MRKO-ob mice compared with FC-ob mice. H: Quantification of PC species based on lipidomic analysis of hepatic lipids from female mice ($n = 4$). Data are presented the same as G. $*P < 0.05$, $**P < 0.01$, $***P < 0.001$. n.s., not significant.

increased in FC-ob mice and attenuated in MRKO-ob mice (Fig. 4A). MRKO-ob mice also had markedly lower hepatic gene expression of *Ly6d* (Fig. 4A), which was reported to be positively associated with hepatic fat content (27,28). Gene
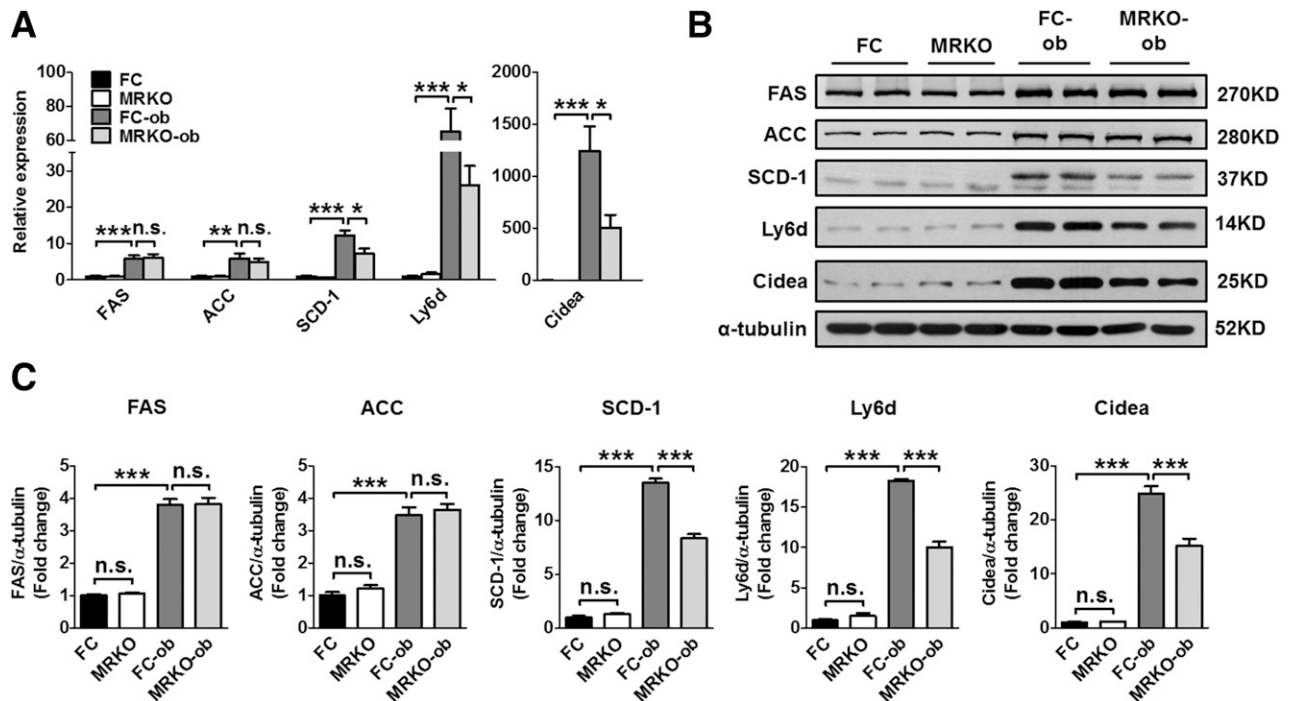
Figure 4—Myeloid MRKO downregulates molecules important in hepatic lipogenesis and lipid storage in female *ob/ob* mice. *A*: qRT-PCR analysis of *FAS, ACC, SCD-1, Ly6d,* and *Cidea* gene expression in liver samples from female mice (*n* = 8). *B*: Immunoblotting analysis of FAS, ACC, SCD-1, Ly6d, and Cidea in liver samples from female mice. *C*: Quantification of immunoblotting results (*n* = 8). *$P < 0.05$, **$P < 0.01$, ***$P < 0.001$. n.s., not significant.

expression of *Cidea* sharply increased in FC-ob mice compared with FC mice and drastically decreased in MRKO-ob mice compared with FC-ob mice (Fig. 4*A*). *Cidea* is a key player in hepatic lipid storage, which is both sufficient and necessary for hepatic steatosis in *ob/ob* mice (29,30). Expression of other lipogenesis-related genes, such as *FAS* and *ACC*, was not affected by MRKO (Fig. 4*A*). Consistent with the results of gene expression, immunoblotting results demonstrated that protein levels of SCD-1, Ly6d, and Cidea were markedly lower in livers of MRKO-ob mice than in FC-ob mice, whereas levels of FAS and ACC were not significantly different between these two genotypes (Fig. 4*B* and *C*). No obvious difference was detected in expression of genes related to β-oxidation or inflammation between FC-ob mice and MRKO-ob mice (Supplementary Fig. 8). These data suggest that myeloid MRKO reduces hepatic lipogenesis and lipid storage in female *ob/ob* mice, contributing to the improvement of hepatic steatosis.
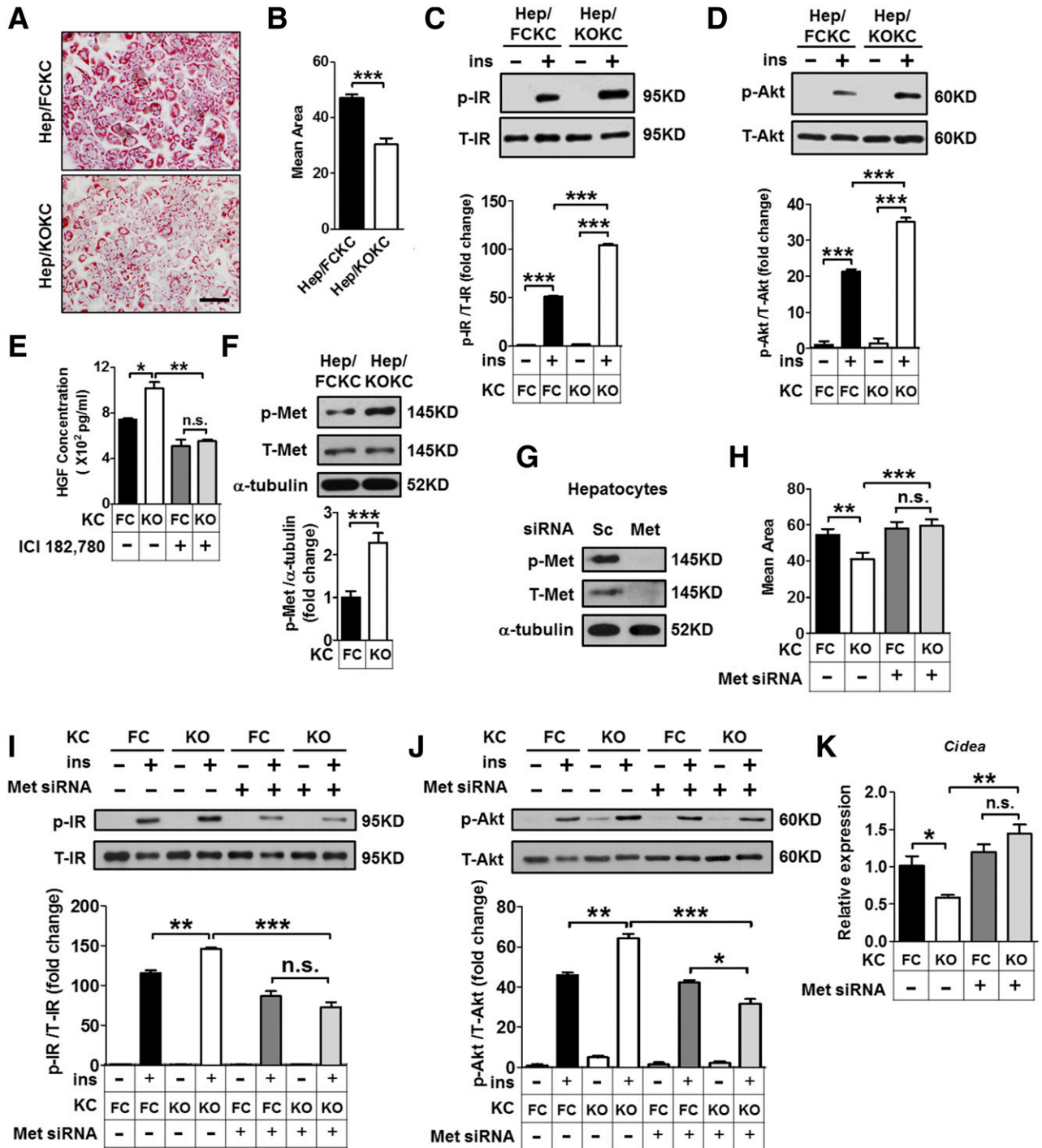
MRKO KCs Reduce Lipid Accumulation and Increase Insulin Sensitivity of Hepatocytes Through an ERα/HGF/Met Axis

Depletion of monocytes/macrophages by using clodronate liposomes abolished the metabolic protection of MRKO and resulted in comparable insulin sensitivity and hepatic lipid content between female FC-ob and female MRKO-ob mice (Supplementary Fig. 9), suggesting that MRKO in

macrophages, but not in other cells of the myeloid lineage, is essential to metabolic protection. We next used KCs, the resident macrophages in the liver, to study their interactions with hepatocytes.

Primary KCs from female FC mice (FCKCs) and KCs from female MRKO mice (KOKCs) were characterized (Supplementary Fig. 10*A–F*) and then cocultured with wild-type primary hepatocytes. Physiological concentration E_2 was added to mimic the microenvironment in females. KOKCs significantly reduced lipid accumulation in hepatocytes compared with FCKCs (Fig. 5*A* and *B*). Staining with BODIPY 493/503 also demonstrated much fewer lipid droplets in the hepatocyte-KOKC coculture system (Supplementary Fig. 10*G*). Furthermore, when cocultured with KOKCs, insulin-induced p-IR and p-Akt were significantly increased in hepatocytes, indicating improved insulin sensitivity (Fig. 5*C* and *D*). Together, these findings demonstrate the protective roles of KOKCs in lipid accumulation and insulin sensitivity of hepatocytes.

HGF, which is secreted by nonparenchymal cells, including macrophages (31), and its receptor Met play essential roles in the maintenance of hepatic insulin sensitivity and glucose homeostasis (32). Of note, when activated by E_2, ER binds to the promoter of *Hgf* to facilitate its expression (33,34). Therefore, we asked whether HGF is associated with the beneficial effects of KOKCs on hepatocytes. Immunofluorescence staining demonstrated that HGF is expressed in KCs (Supplementary Fig. 11*A*). Depletion of

Figure 5—MR deficiency in KCs reduces lipid accumulation and increases insulin sensitivity in hepatocytes through the ERα/HGF/Met pathway. *A*: Oil Red O staining of hepatocytes cocultured with FCKC or KOKC in the presence of FFAs and E$_2$. Scale bar = 200 μm. *B*: Quantification of Oil Red O staining. *C*: Immunoblotting analysis and quantification of p-IR in hepatocytes from the above-described coculture system. *D*: Immunoblotting analysis and quantification of p-Akt (Ser473) in hepatocytes from the above-described coculture system. *E*: ELISA analysis of HGF in supernatants of FCKCs and KOKCs in the presence of FFAs and E$_2$. *F*: Immunoblotting analysis and quantification of phosphorylated Met (p-Met) in hepatocytes cocultured with FCKCs or KOKCs in the presence of FFAs and E$_2$. *G*: Immunoblotting analysis of p-Met and total Met (T-Met) in hepatocytes after transfection with scrambled siRNA or Met siRNA. Cells were stimulated with 40 ng/mL HGF for 15 min before collection. *H*: Quantification of Oil Red O staining of hepatocytes transfected with scrambled siRNA (−) or Met siRNA (+) followed by coculture with FCKCs or KOKCs in the presence of E$_2$ and FFAs. *I*: Immunoblotting analysis and quantification of p-IR in hepatocytes from the coculture system in *H*. *J*: Immunoblotting analysis and quantification of p-Akt (Ser473) in hepatocytes from the coculture system in *H*. *K*: qRT-PCR analysis of *Cidea* gene expression in hepatocytes from the coculture system in *H*. Data are from three independent experiments. *$P < 0.05$, **$P < 0.01$, ***$P < 0.001$. Hep, hepatocytes; −, before insulin injection; +, after insulin injection; n.s., not significant; Sc, scrambled.

monocytes/macrophages by using clodronate liposomes significantly decreased HGF secretion in nonparenchymal cells from livers and erased the difference between female FC-ob and MRKO-ob mice, suggesting that KCs are a major source of HGF in the liver (Supplementary Fig. 11B). In the presence of E_2 and FFAs, KOKCs secreted more HGF than FCKCs, and the upregulation was blocked by ICI 182,780, an antagonist of ERα, suggesting that ERα mediates these effects (Fig. 5E). Knockdown of ERα also blocked the increase of HGF secretion in KOKCs (Supplementary Fig. 11C and D). Conversely, overexpression of ERα increased HGF secretion in KCs (Supplementary Fig. 11E and F).

Phosphorylation of Met (p-Met) (HGF receptor) was enhanced in hepatocytes cocultured with KOKCs compared with those cocultured with FCKCs in the presence of E_2 (Fig. 5F). Knockdown of Met in hepatocytes by using siRNA (Fig. 5G) blocked the impacts of KOKCs on the reduction of lipid accumulation in hepatocytes (Fig. 5H). Furthermore, enhanced insulin signaling in hepatocytes cocultured with KOKCs was abolished by Met knockdown (Fig. 5I and J). In parallel, the downregulation of *Cidea* gene expression in hepatocytes cocultured with KOKCs was also blocked by Met knockdown (Fig. 5K). Taken together, these data indicate that an ERα/HGF/Met axis plays an indispensable role in mediating the beneficial effects of KOKCs on the metabolic improvements of hepatocytes.

MR Directly Regulates *Esr1* in Macrophages

Results of qRT-PCR showed that expression of *Esr1* (encoding ERα) significantly increased in KOKCs (Fig. 6A). Conversely, RAW264.7 cells with stable MROV (Supplementary Fig. 12A and B) had much lower expression of *Esr1* (Fig. 6B). These data indicate repressive regulation of *Esr1* by MR in macrophages.

Five putative MR response elements (MREs) were identified in the promoter region of mouse *Esr1* (hereafter referred as region 1~5, or R1~5) (Fig. 6C). Truncated *Esr1* promoters containing a gradually decreasing number of the predicted MREs (omission starting from R1) were constructed to perform luciferase reporter assay in HEK293FT cells (Fig. 6D). HEK293FT cells transfected with MR-flag plasmid were cultured with charcoal/dextran-treated serum, and detectable MR-flag was localized in the nuclei, suggesting ligand-independent nuclear accumulation (Supplementary Fig. 12C). Cotransfection experiments showed that expression of MR-flag suppressed the transcription of all *Esr1* promoters with different lengths (Fig. 6E). In particular, these results indicated that both R5 alone and R4~5 were sufficient for MR to suppress *Esr1* transcription and that R1~3 were not necessary (Fig. 6E). Another group of truncated *Esr1* promoters containing a gradually decreasing number of the predicted MREs (omission starting from R5) were constructed (Fig. 6F). MR-flag still decreased the transcription of *Esr1* promoter when R5 was absent, suggesting that R5 was not necessary for the suppression (Fig. 6G). However, the suppression disappeared when both R4 and R5 were absent, suggesting that R4 was required and that

R1~3 was not sufficient (Fig. 6G). Together, these results suggest that functional MREs are located in R4 and/or R5. Subsequently, a ChIP assay using the MROV RAW264.7 cells demonstrated direct binding of MR to *Esr1* promoter in R4 and R5, but not R1~3, further supporting the functionality of the MREs in R4 and R5 (Fig. 6H and I).

### Hepatic Met Mediates the Beneficial Effects of Myeloid MR Deficiency in Female *ob/ob* Mice

Knockdown of Met in livers was carried out by using adenoviruses expressing Met-specific shRNA (AdshMet) (Supplementary Fig. 13). Injection of AdshMet abolished the protective effects of MRKO on random-fed blood glucose, fasting plasma insulin level, GTT, and ITT in female *ob/ob* mice (Fig. 7A–D). Similarly, adenovirus expressing scrambled shRNA (AdshScr) eliminated the beneficial impacts of MRKO on LW/BW, hepatic TG content, hepatic lipid accumulation, and hepatic p-IR and p-Akt in female *ob/ob* mice (Fig. 7E–I). Together, these results strongly suggest that MR deficiency improves glucose homeostasis, insulin sensitivity, and hepatic lipid metabolism and insulin signaling, depending on hepatic Met in vivo. We propose a working model to illustrate the MR/ERα/HGF/Met axis that mediates the interactions between macrophages and hepatocytes in the liver and that may explain the impacts of MRKO on insulin resistance and hepatic steatosis (Fig. 7J).

DISCUSSION

Although the function of MR in electrolyte balance and the cardiovascular system has been investigated in more detail, much less has been studied in glucose and lipid metabolism. Through the current study, we uncovered the beneficial effects of myeloid-specific MR blockade on hepatic lipid metabolism as well as systemic insulin sensitivity and glucose homeostasis in *ob/ob* mice. We also identified a novel mechanism through which MR and ERα cross talk and macrophage and hepatocytes communicate to regulate lipid accumulation and insulin sensitivity.

Estrogen Is Both Sufficient and Necessary for the Metabolic Improvements of Myeloid MR Deficiency in Obese Mice

We demonstrate that myeloid MRKO protected female obese mice against glucose intolerance, insulin resistance, and hepatic steatosis. Although female *ob/ob* mice are infertile (35), a fair amount of E_2 is detected in these mice according to the current results and other reports (36). In addition, ovaries of *ob/ob* mice are capable of producing viable eggs when transplanted into lean female recipients (37), suggesting functional ovarian hormones, including estrogen, in these mice. The results further show that OVX abolished the protective effects of myeloid MRKO in female obese mice and that estrogen supplementation to male obese mice was sufficient to bring out the metabolic protection of myeloid MRKO, illustrating the sufficiency and requirement of estrogen. The metabolic protection of estrogen signaling has been well documented in both human subjects and animal models (38). In particular, estrogen
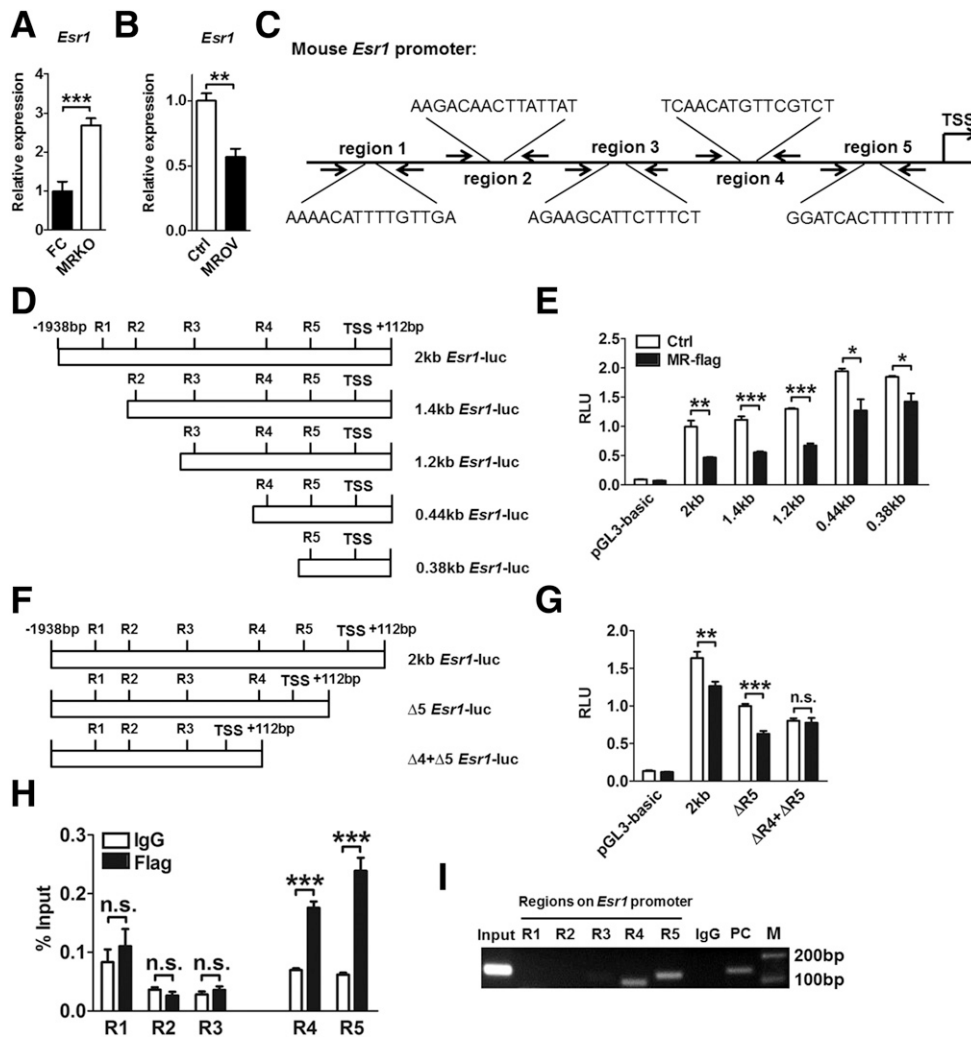
Figure 6—MR directly regulates *Esr1* in macrophages. *A*: qRT-PCR analysis of *Esr1* gene expression in FCKCs and KOKCs in the presence of E₂. *B*: qRT-PCR analysis of *Esr1* gene expression in stable MROV RAW264.7 cells. *C*: Schematic illustration of the five putative MREs on mouse *Esr1* promoter. MREs are labeled by region 1~5. Arrows flanking each region represent locations of specific primers. *D* and *F*: Schematic illustrations of luciferase reporter constructs containing truncated mouse *Esr1* promoters with various numbers of putative MREs (R1~ R5). *E* and *G*: Luciferase reporter assays using HEK293FT cells cotransfected with MR-flag plasmid or empty vector (Ctrl) and truncated *Esr1* promoter luciferase reporter plasmids (*Esr1*-luc) or control plasmid pGL3-basic. *H*: qRT-PCR analysis of ChIP products. ChIP was performed by using stable MROV RAW264.7 cells. Antibody against FLAG or IgG was used for immunoprecipitation. *I*: Gel electrophoresis image of regular PCR products with use of the ChIP products. R1~ R5, amplification of ChIP products pulled down with anti-FLAG antibody (primers were specific to R1~ R5, respectively). Data are from three independent experiments. *$P < 0.05$, **$P < 0.01$, ***$P < 0.001$. bp, base pair; M, 100-base pair DNA ladder; n.s., not significant; PC, positive control with primers specific to mouse *Sgk1* (a known target gene of MR) promoter; RLU, relative luciferase unit; TSS, transcription start site.

signaling in myeloid cells has been reported to exert a critical function in metabolic regulation (39). Previous reports have demonstrated protective impacts of enhanced estrogen signaling on glucose and lipid metabolism in *ob/ob* mice (40). The current study illustrates that the combination of estrogen and myeloid MR deficiency is effective at improving insulin resistance and hepatic steatosis.

The MR/ERα/HGF/Met Signaling Axis Facilitates Macrophage-Hepatocyte Interaction

The data suggest that MR deficiency in macrophages is mainly responsible for the metabolic improvements of MRKO in obese mice, although the relative contribution of resident KCs and infiltrated macrophages remain to be investigated. Previous studies have revealed that hepatocyte-derived interleukin-4 and interleukin-13 are important determinants of macrophage phenotype (15,41). We conversely identified an MR/ERα/HGF/Met pathway that controlled metabolic signal transduction from macrophages to hepatocytes and ultimately contributed to metabolic regulation in the liver. HGF/Met is an important pair in the regulation of hepatic insulin sensitivity and glucose homeostasis (32). Specific deletion of Met in hepatocytes leads to the development of severe nonalcoholic steatohepatitis in mice (42). We demonstrated that in macrophages, MR directly regulated the expression of ERα, which in turn controlled
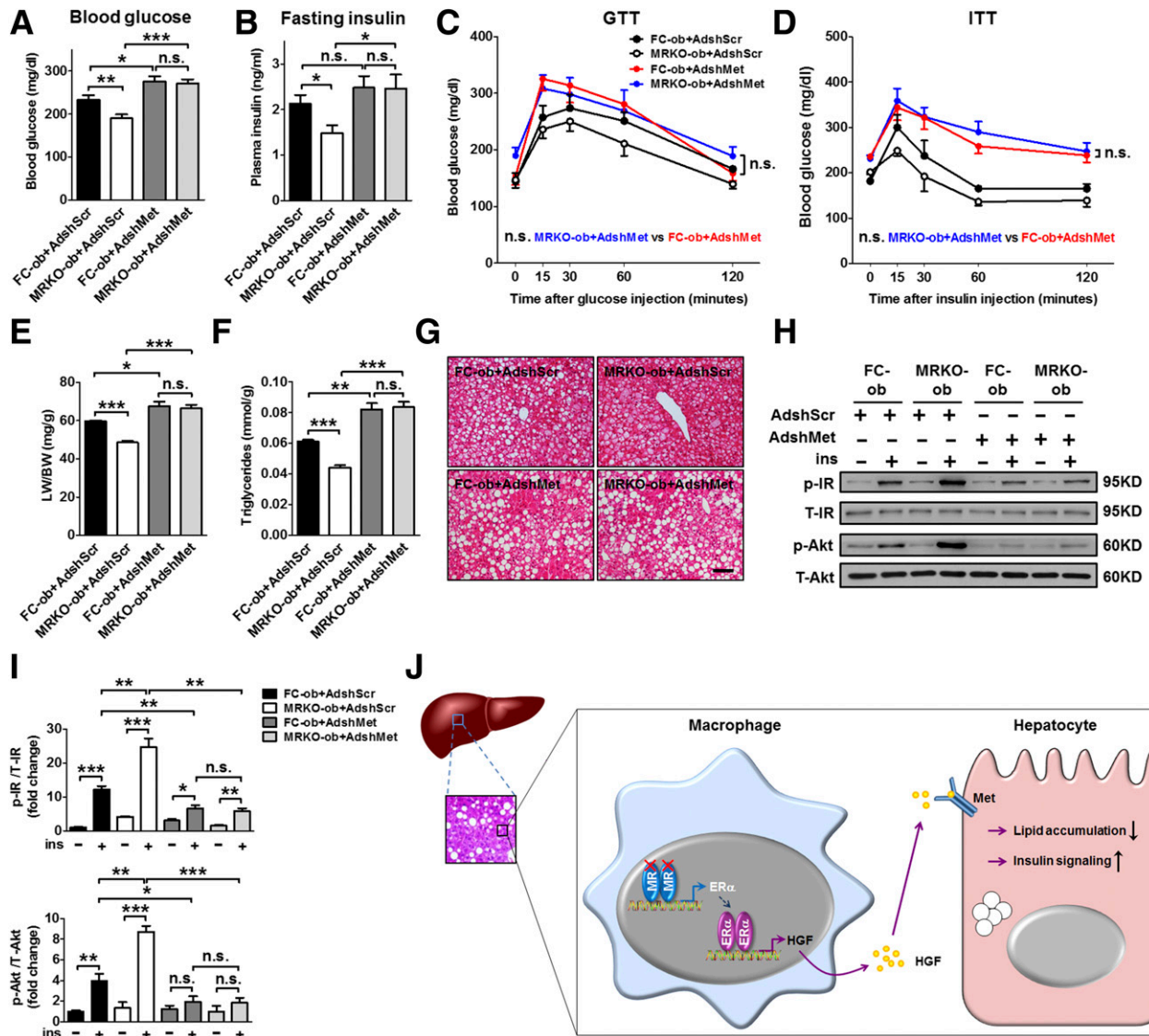
Figure 7—Hepatic Met mediates the protective effects of myeloid MR deficiency in vivo. A and B: Random-fed blood glucose and fasting plasma insulin levels of female FC-ob and MRKO-ob mice injected with AdshScr or AdshMet. C–G: GTT, ITT, LW/BW, hepatic TGs, and hepatic H&E staining of female FC-ob and MRKO-ob mice injected with AdshScr or AdshMet. Scale bar = 400 μm. H: Immunoblotting analysis of p-IR, total IR (T-IR), p-Akt (Ser473), and total Akt (T-Akt) in livers of female FC-ob and MRKO-ob mice injected with AdshScr or AdshMet before and after insulin injection. I: Quantifications of immunoblotting results as p-IR/T-IR and p-Akt/T-Akt. J: Working model of the MR/ERα/HGF/Met axis that conveys metabolic signaling from macrophages to hepatocytes. In the liver where macrophages and hepatocytes are situated in proximity, MR deficiency leads to elevated ERα expression followed by enhanced HGF secretion from macrophages in the presence of estrogen. HGF subsequently phosphorylates and activates hepatocyte Met, which mediates the decrease of lipid accumulation and the increase of insulin signaling in hepatocytes and improves hepatic steatosis and insulin resistance in female and E₂-implanted male ob/ob mice. n = 6–10. *P < 0.05, **P < 0.01, ***P < 0.001. −, before insulin injection; +, after insulin injection; n.s., not significant.

the release of HGF that binds to Met on hepatocytes. Through such communications, MRKO in macrophages decreases lipid accumulation and improves insulin sensitivity in hepatocytes. We also observed that macrophage MRKO downregulated critical lipid-regulating molecules, such as *Cidea*, in hepatocytes depending of Met, implying that these molecules were downstream of the MR/ERα/HGF/Met pathway. However, the exact mechanism for how this signaling pathway controls these molecules remains to be interrogated.

We mainly used *ob/ob* mice as the obese mouse model to explore the roles of myeloid MR in hepatic steatosis and insulin resistance. Although widely used in metabolic studies, *ob/ob* mice possess several limitations. In particular, leptin mutation and deficiency are not a common cause of NAFLD or T2DM in humans, wherein the etiology is much more complex. Our study characterizes the MR/ERα/HGF/Met axis as a potentially important metabolic pathway in connecting macrophages to hepatocytes. Future work to test the metabolic consequence of MR blockade in human subjects or cells may provide more translatable insights into human NAFLD and T2DM.

Nuclear Receptor-Nuclear Receptor Cross Talk Controls Hepatic Metabolism

Nuclear receptors are important hubs of transcriptional control, and their target genes include those critical in metabolic regulation (43,44). Their functions in maintaining metabolic homeostasis are further amplified or fine-tuned by nuclear receptor-nuclear receptor cross talk. The mutual inhibition between peroxisome proliferator–activated receptor-α and liver X receptor is a good example (45,46). Through reciprocal regulations, these two nuclear receptors put hepatic lipid metabolism under balanced control (45,46). A previous study demonstrated that MR and ERα physically interact with each other in HEK293 cells (47). Furthermore, ERα activation has been shown to inhibit MR-mediated gene expression (47). The current results identify ERα as a target gene of MR. In macrophages, MR regulates ERα, which itself plays key roles in metabolic regulation and, in this case, mediates the secretion of HGF to deliver messages from macrophages to hepatocytes. All these data support the importance of cross talk between nuclear receptors in metabolic regulation.

Conclusions

In summary, we identified an MR/ERα/HGF/Met signaling pathway that mediates MR-ERα cross talk and macrophage-hepatocyte interaction and that ultimately conveys the protective effects of myeloid MR deficiency on glucose homeostasis, insulin sensitivity, and hepatic lipid metabolism in obese mice. These findings may have opened a new window to explore the functions of MR in metabolic regulation. Perturbation of macrophage MR, with or without supplementation of estrogen, may be a potential novel strategy to fight against NAFLD and T2DM.

References

1. Rinella ME. Nonalcoholic fatty liver disease: a systematic review. JAMA 2015;313:2263–2273

2. Byrne CD, Targher G. NAFLD: a multisystem disease. J Hepatol 2015; 62(Suppl.):S47–S64

3. Huang W, Metlakunta A, Dedousis N, et al. Depletion of liver Kupffer cells prevents the development of diet-induced hepatic steatosis and insulin resistance. Diabetes 2010;59:347–357

4. Hotamisligil GS. Inflammation and metabolic disorders. Nature 2006;444:860–867

5. De Taeye BM, Novitskaya T, McGuinness OP, et al. Macrophage TNF-alpha contributes to insulin resistance and hepatic steatosis in diet-induced obesity. Am J Physiol Endocrinol Metab 2007;293:E713–E725

6. Lother A, Moser M, Bode C, Feldman RD, Hein L. Mineralocorticoids in the heart and vasculature: new insights for old hormones. Annu Rev Pharmacol Toxicol 2015;55:289–312

7. Ferrario CM, Schiffrin EL. Role of mineralocorticoid receptor antagonists in cardiovascular disease. Circ Res 2015;116:206–213

8. Yancy CW, Jessup M, Bozkurt B, et al. 2013 ACCF/AHA guideline for the management of heart failure: executive summary: a report of the American College of Cardiology Foundation/American Heart Association Task Force on practice guidelines. Circulation 2013;128:1810–1852

9. Guo C, Ricchiuti V, Lian BQ, et al. Mineralocorticoid receptor blockade reverses obesity-related changes in expression of adiponectin, peroxisome proliferator-activated receptor-gamma, and proinflammatory adipokines. Circulation 2008;117:2253–2261

10. Hirata A, Maeda N, Hiuge A, et al. Blockade of mineralocorticoid receptor reverses adipocyte dysfunction and insulin resistance in obese mice. Cardiovasc Res 2009;84:164–172

11. Wada T, Kenmochi H, Miyashita Y, et al. Spironolactone improves glucose and lipid metabolism by ameliorating hepatic steatosis and inflammation and suppressing enhanced gluconeogenesis induced by high-fat and high-fructose diet. Endocrinology 2010;151:2040–2049

12. Pizarro M, Solis N, Quintero P, et al. Beneficial effects of mineralocorticoid receptor blockade in experimental non-alcoholic steatohepatitis. Liver Int 2015; 35:2129–2138

13. Usher MG, Duan SZ, Ivaschenko CY, et al. Myeloid mineralocorticoid receptor controls macrophage polarization and cardiovascular hypertrophy and remodeling in mice. J Clin Invest 2010;120:3350–3364

14. Dabrosin C, Gyorffy S, Margetts P, Ross C, Gauldie J. Therapeutic effect of angiostatin gene transfer in a murine model of endometriosis. Am J Pathol 2002; 161:909–918

15. Odegaard JI, Ricardo-Gonzalez RR, Red Eagle A, et al. Alternative M2 activation of Kupffer cells by PPARdelta ameliorates obesity-induced insulin resistance. Cell Metab 2008;7:496–507

16. Sun JY, Li C, Shen ZX, et al. Mineralocorticoid receptor deficiency in macrophages inhibits neointimal hyperplasia and suppresses macrophage inflammation through SGK1-AP1/NF-κB Pathways. Arterioscler Thromb Vasc Biol 2016;36:874–885

17. Mehlem A, Hagberg CE, Muhl L, Eriksson U, Falkevall A. Imaging of neutral lipids by Oil Red O for analyzing the metabolic status in health and disease. Nat Protoc 2013;8:1149–1154

18. Liu Y, Zhou D, Zhang F, et al. Liver Patt1 deficiency protects male mice from age-associated but not high-fat diet-induced hepatic steatosis. J Lipid Res 2012; 53:358–367

19. Han X, Yang J, Cheng H, Ye H, Gross RW. Toward fingerprinting cellular lipidomes directly from biological samples by two-dimensional electrospray ionization mass spectrometry. Anal Biochem 2004;330:317–331

20. Han X, Yang K, Cheng H, Fikes KN, Gross RW. Shotgun lipidomics of phosphoethanolamine-containing lipids in biological samples after one-step in situ derivatization. J Lipid Res 2005;46:1548–1560

21. Yang K, Cheng H, Gross RW, Han X. Automated lipid identification and quantification by multidimensional mass spectrometry-based shotgun lipidomics. Anal Chem 2009;81:4356–4368

22. Wang Q, Jiang L, Wang J, et al. Abrogation of hepatic ATP-citrate lyase protects against fatty liver and ameliorates hyperglycemia in leptin receptor-deficient mice. Hepatology 2009;49:1166–1175

23. Froh M, Konno A, Thurman RG. Isolation of liver Kupffer cells. Curr Protoc Toxicol 2003;Chapter 14:Unit14.4

24. Yan S, Zhang Q, Zhong X, et al. I prostanoid receptor-mediated inflammatory pathway promotes hepatic gluconeogenesis through activation of PKA and inhibition of AKT. Diabetes 2014;63:2911–2923

25. Pettersson US, Waldén TB, Carlsson PO, Jansson L, Phillipson M. Female mice are protected against high-fat diet induced metabolic syndrome and increase the regulatory T cell population in adipose tissue. PLoS One 2012;7: e46057

26. Miyazaki M, Flowers MT, Sampath H, et al. Hepatic stearoyl-CoA desaturase-1 deficiency protects mice from carbohydrate-induced adiposity and hepatic steatosis. Cell Metab 2007;6:484–496

27. Guillén N, Navarro MA, Arnal C, et al. Microarray analysis of hepatic gene expression identifies new genes involved in steatotic liver. Physiol Genomics 2009;37:187–198

28. Kang HS, Liao G, DeGraff LM, et al. CD44 plays a critical role in regulating diet-induced adipose inflammation, hepatic steatosis, and insulin resistance. PLoS One 2013;8:e58417

29. Zhou Z, Yon Toh S, Chen Z, et al. Cidea-deficient mice have lean phenotype and are resistant to obesity. Nat Genet 2003;35:49–56

30. Zhou L, Xu L, Ye J, et al. Cidea promotes hepatic steatosis by sensing dietary fatty acids. Hepatology 2012;56:95–107

31. D'Angelo F, Bernasconi E, Schäfer M, et al. Macrophages promote epithelial repair through hepatocyte growth factor secretion. Clin Exp Immunol 2013;174: 60–72

32. Fafalios A, Ma J, Tan X, et al. A hepatocyte growth factor receptor (Met)-insulin receptor hybrid governs hepatic glucose metabolism. Nat Med 2011;17: 1577–1584

33. Liu Y, Lin L, Zarnegar R. Modulation of hepatocyte growth factor gene expression by estrogen in mouse ovary. Mol Cell Endocrinol 1994;104: 173–181

34. Jiang JG, Bell A, Liu Y, Zarnegar R. Transcriptional regulation of the hepatocyte growth factor gene by the nuclear receptors chicken ovalbumin upstream promoter transcription factor and estrogen receptor. J Biol Chem 1997; 272:3928–3934

35. Coleman DL. Obese and diabetes: two mutant genes causing diabetes-obesity syndromes in mice. Diabetologia 1978;14:141–148

36. Gao J, He J, Shi X, et al. Sex-specific effect of estrogen sulfotransferase on mouse models of type 2 diabetes. Diabetes 2012;61:1543–1551

37. Batt RA. The response of the reproductive system in the female mutant mouse, obese (genotype obob) to gonadotrophin-releasing hormones. J Reprod Fertil 1972;31:496–497

38. Mauvais-Jarvis F. Estrogen and androgen receptors: regulators of fuel homeostasis and emerging targets for diabetes and obesity. Trends Endocrinol Metab 2011;22:24–33

39. Ribas V, Drew BG, Le JA, et al. Myeloid-specific estrogen receptor alpha deficiency impairs metabolic homeostasis and accelerates atherosclerotic lesion development. Proc Natl Acad Sci U S A 2011;108:16457–16462

40. Jiang M, He J, Kucera H, et al. Hepatic overexpression of steroid sulfatase ameliorates mouse models of obesity and type 2 diabetes through sex-specific mechanisms. J Biol Chem 2014;289:8086–8097

41. Kang K, Reilly SM, Karabacak V, et al. Adipocyte-derived Th2 cytokines and myeloid PPARdelta regulate macrophage polarization and insulin sensitivity. Cell Metab 2008;7:485–495

42. Kroy DC, Schumacher F, Ramadori P, et al. Hepatocyte specific deletion of c-Met leads to the development of severe non-alcoholic steatohepatitis in mice. J Hepatol 2014;61:883–890

43. Rando G, Wahli W. Sex differences in nuclear receptor-regulated liver metabolic pathways. Biochim Biophys Acta 2011;1812:964–973

44. Evans RM, Mangelsdorf DJ. Nuclear receptors, RXR, and the big bang. Cell 2014;157:255–266

45. Yoshikawa T, Ide T, Shimano H, et al. Cross-talk between peroxisome proliferator-activated receptor (PPAR) alpha and liver X receptor (LXR) in nutritional regulation of fatty acid metabolism. I. PPARs suppress sterol regulatory element binding protein-1c promoter through inhibition of LXR signaling. Mol Endocrinol 2003;17:1240–1254

46. Ide T, Shimano H, Yoshikawa T, et al. Cross-talk between peroxisome proliferator-activated receptor (PPAR) alpha and liver X receptor (LXR) in nutritional regulation of fatty acid metabolism. II. LXRs suppress lipid degradation gene promoters through inhibition of PPAR signaling. Mol Endocrinol 2003;17: 1255–1267

47. Barrett Mueller K, Lu Q, Mohammad NN, et al. Estrogen receptor inhibits mineralocorticoid receptor transcriptional regulatory function. Endocrinology 2014; 155:4461–4472